UNIVERSITÉ DE GENÈVE

Archive ouverte UNIGE
https://archive-ouverte.unige.ch

Article scientifique | Article | 2012

Published version | Open Access

This is the published version of the publication, made available in accordance with the publisher's policy.

O-glycosylated IgA rheumatoid factor induces IgA deposits and glomerulonephritis

Otani, Masako; Nakata, Junichiro; Kihara, Masao; Leroy, Valérie; Moll, Solange; Wada, Yoshinao; Izui, Shozo

How to cite

OTANI, Masako et al. O-glycosylated IgA rheumatoid factor induces IgA deposits and glomerulonephritis. In: Journal of the American Society of Nephrology, 2012, vol. 23, n° 3, p. 438–446. doi: 10.1681/ASN.2011070701

This publication URL: https://archive-ouverte.unige.ch/unige:43826
Publication DOI: 10.1681/ASN.2011070701

© This document is protected by copyright. Please refer to copyright holder(s) for terms of use.

O-Glycosylated IgA Rheumatoid Factor Induces IgA Deposits and Glomerulonephritis

Masako Otani,* Junichiro Nakata,† Masao Kihara,† Valérie Leroy,* Solange Moll,* Yoshinao Wada,‡ and Shozo Izui*

*Department of Pathology and Immunology, University of Geneva, Geneva, Switzerland; †Division of Nephrology, Department of Internal Medicine, Juntendo University Faculty of Medicine, Tokyo, Japan; and ‡Department of Molecular Medicine, Osaka Medical Center and Research Institute for Maternal and Child Health, Osaka, Japan

ABSTRACT

Structural aberrations of *O*-linked glycans present in the IgA1 hinge region are associated with IgA nephropathy, but their contribution to its pathogenesis remains incompletely understood. In this study, mice implanted with hybridoma secreting 6-19 IgA anti-IgG2a rheumatoid factor, but not 46-42 IgA rheumatoid factor bearing the same IgA allotype, developed mesangial deposits consisting of IgA, IgG2a, and C3. Studies in immunoglobulin- and C3-deficient mice revealed that the development of these glomerular lesions required the formation of IgA-IgG2a immune complexes and subsequent activation of complement. The proportion of polymeric and monomeric forms, the IgG2a-binding affinity, and the serum levels of IgA-IgG2a immune complexes were similar between 6-19 IgA– and 46-42 IgA–injected mice. In contrast, the analysis of oligosaccharide structures revealed highly galactosylated *O*-linked glycans in the hinge region of 6-19 IgA and poorly *O*-glycosylated in the hinge region of 46-42 IgA. Furthermore, the structure of *N*-linked glycans in the CH1 domain was the complex type in 6-19 IgA and the hybrid type in 46-42 IgA. In summary, this study demonstrates the presence of *O*-linked glycans in the hinge region of mouse IgA and suggests that 6-19 IgA rheumatoid factor–induced GN could serve as an experimental model for IgA nephropathy.

J Am Soc Nephrol 23: 438–446, 2012. doi: 10.1681/ASN.2011070701

IgA nephropathy (IgAN) is the most common form of GN. It has a variable spectrum of clinical presentations and leads to progressive renal failure in almost one third of patients.[1] The glomerular lesions are characterized by immune deposits of IgA in the mesangium and by mesangial cell proliferation and expansion of extracellular matrix. IgA deposits are usually accompanied by deposition of the C3 component of complement and by variable co-deposition of IgG and/or IgM. Most significantly, mesangial immune deposits are restricted to the IgA1 subclass, not the IgA2 subclass.[2]

The most prominent structural difference between IgA1 and IgA2 is the presence of as many as five *O*-linked oligosaccharide side chains in the hinge region of IgA1, but not in IgA2.[3] *O*-linked glycans (*O*-glycans) of IgA1 are synthesized through the attachment of *N*-acetylgalactosamine (GalNAc) to serine or threonine residue, which is then extended by sequential attachment of galactose (Gal) or sialic acid residues to GalNAc. The prevailing forms of the carbohydrate composition of *O*-glycans in the IgA1 hinge region include GalNAc-Gal disaccharide and its mono- and disialylated forms. In contrast, Gal-deficient variants are much more common in patients with IgAN and are predominantly found in circulating immune complexes and glomerular immune deposits.[4–7] Therefore, it has been suggested that hypogalactosylation of the *O*-glycans in the IgA1 hinge region and the subsequent development of IgA1 complexes are critically involved in the pathogenesis of IgAN.

Received July 19, 2011. Accepted October 19, 2011.

Published online ahead of print. Publication date available at www.jasn.org.

Correspondence: Dr. Shozo Izui, Department of Pathology and Immunology, Centre Médical Universitaire, 1211 Geneva 4, Switzerland. Email: Shozo.Izui@unige.ch

Copyright © 2012 by the American Society of Nephrology

The pathogenic mechanism contributed by the undergalactosylation of IgA1, as well as the underlying defect responsible for reduced galactosylation of *O*-glycans of IgA1, remain largely unknown. This is in part due to the absence of appropriate mouse models of IgAN. Indeed, it has been believed that *O*-glycans are absent in the hinge region of murine IgA, as reported after the structural analysis of oligosaccharide chains from two different monoclonal IgAs derived from BALB/c mice bearing the *Igh-2*^{a} allotype.[8,9] However, because studies on human IgA1 and hemopexin revealed that the occupancy of the *O*-linked glycosylation site is usually partial,[10,11] the possible presence of *O*-glycans in a fraction of murine IgA cannot be totally excluded. Indeed, the presence of a potential *O*-linked glycosylation site has been suggested in the hinge region of murine IgA bearing the *Igh-2*^{a} and *Igh-2*^{c} allotypes.[12] In contrast, murine IgA carries at least two *N*-linked oligosaccharide side chains in CH1 and CH3 domains,[8,9,13] and Gal deficiency of *N*-linked glycans (*N*-glycans) has been reported to be associated with the development of glomerular lesions in murine models of IgAN.[14–16]

In the present study, we explored the nephritogenic potential of two different monoclonal IgA anti-IgG2a rheumatoid factors (RFs) bearing the *Igh-2*^{a} allotype (6-19 and 46-42) in relation to the possible presence of *O*-glycans in their hinge regions and to the structural abnormality of *N*-glycans in their CH1 and CH3 domains. We observed that only 6-19 IgA RF mAb carrying *O*-glycans in the hinge region is able to induce severe glomerular lesions characterized by mesangial IgA deposits, although its *O*-glycans are highly galactosylated, and that the structure of *N*-glycans present in the CH1 domain of 6-19 IgA RF is also markedly different from that of non-nephritogenic 46-42 IgA RF.

RESULTS

Induction of Glomerular Lesions by 6-19 but Not 46-42 IgA Anti-IgG2a RF mAb in BALB/c Mice

Previous research has shown that 6-19 IgG3 anti-IgG2a RF mAb derived from lupus-prone MRL-*Fas*^{lpr} mice induces "wire-loop"–like glomerular lesions characterized by subendothelial deposits.[17] Because the pathogenicity of 6-19 IgG3 RF depends on the IgG3 subclass,[18] which has the unique physiochemical property of generating self-associating complexes,[19] a polymeric form of an IgA variant of 6-19 RF mAb could induce glomerular lesions resembling those observed in human IgAN. We therefore generated an IgA class-switch variant of 6-19 RF mAb and explored its nephritogenic potential in BALB/c mice.

After intraperitoneal implantation of 6-19 IgA RF transfectoma cells, serum levels of IgA RF progressively increased and significant amounts of IgA-IgG2a immune complexes were detectable in sera (Figure 1 and Table 1). Two to three weeks later, BALB/c mice developed severe glomerular lesions, characterized by segmental expansion of mesangial cell matrix and mesangial cell proliferation in the majority of glomeruli, infiltration of PMNs in some glomeruli, and sclerotic changes in far advanced cases (Figure 2A and Supplemental Figure 1).

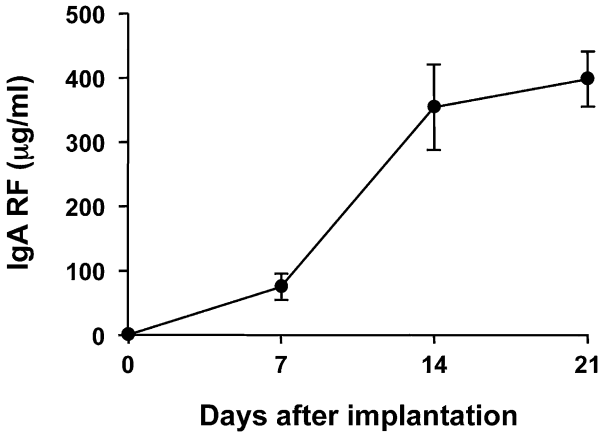

Figure 1. Serum levels of IgA anti-IgG2a in BALB/c mice implanted with 6-19 IgA anti-IgG2a RF–secreting cells. A total of 10^7 6-19 IgA RF–secreting transfectoma cells were intraperitoneally injected into 2-month-old BALB/c mice. Serum levels of IgA anti-IgG2a (mean values from mice ± SEM) are expressed as μg/ml. One representative experiment out of two independent experiments (five mice per group for each experiment) is shown.

Immunofluorescence analysis revealed massive deposits of IgA, IgG2a, and C3 in the mesangium (Figure 2B), and the mesangial localization of immune deposits was confirmed by electron microscopic analysis (Figure 2C). In parallel, serum levels of BUN were significantly elevated ($P<0.01$; Table 1), although creatinine levels (0.25±0.04 mg/dl) remained similar to those before implantation of 6-19 IgA cells (0.17±0.03 mg/dl). In contrast, no substantial histologic alterations were observed in glomeruli of mice implanted with 46-42 IgA anti-IgG2a RF hybridoma cells (Figure 2D and Supplemental Figure 1). These glomeruli displayed only minimal deposits of IgA and IgG2a, without detectable C3, in the mesangium, consistent with lack of increases in BUN levels in these mice (Table 1). Notably, serum levels of IgA anti-IgG2a RF and IgA-IgG2a immune complexes were even higher in mice implanted with 46-42 hybridoma cells than in mice implanted with 6-19 IgA RF cells (Table 1). These results indicate that 6-19 IgA RF exhibited a unique pathogenic potential to induce glomerular lesions resembling those observed in human IgAN.

Lack of Induction of Glomerular Lesions by 6-19 IgA Anti-IgG2a RF mAb in Immunoglobulin- and C3-Deficient BALB/c Mice

To determine whether the immune complex formation between 6-19 IgA anti-IgG2a and IgG2a could be involved in the development of 6-19 IgA–induced glomerular lesions, 6-19 IgA transfectoma cells were implanted into immunoglobulin-deficient BALB/c mice. We observed that immunoglobulin-deficient mice, which

Table 1. Serum levels of IgA anti-IgG2a RF and development of glomerular lesions in BALB/c mice implanted with 6-19 IgA RF–secreting transfectoma cells

IgA[a]	Mice[a]	IgA Anti-IgG2a (μg/ml)[b]	IgA-IgG2a Immune Complex (OD)[c]	BUN (mg/dl)[d]	Incidence of Glomerular Lesions (*n*/*n*)[e]
6-19	WT	397.4±30.2	0.365±0.039	39.0±3.9	10/10
	$Ig^{-/-}$	475.4±53.2	NT	24.5±1.6	0/12
	$C3^{-/-}$	358.0±52.8	NT	23.0±0.9	0/12
46-42	WT	626.3±27.4	0.528±0.062	27.3±2.0	0/15

Values expressed with a plus/minus sign are the mean ± SEM. WT, wild type.
[a]10^7 6-19 or 46-42 IgA RF–secreting cells were inoculated intraperitoneally into 2-month-old WT, immunoglobulin- or C3-deficient BALB/c mice.
[b]Serum levels of IgA anti-IgG2a RF 3 weeks after implantation of 6-19 or 46-42 IgA RF–secreting cells, expressed as μg/ml (mean of 10–15 mice ± SEM; pooled results from 2–3 independent experiments with 5–7 mice per group for each experiment). Serum levels of IgA anti-IgG2a before injection of cells were less than 1 μg/ml.
[c]Serum levels of IgA-IgG2a immune complexes 3 weeks after implantation of 6-19 or 46-42 IgA RF–secreting cells, expressed as OD at 405 nm (mean of 10 mice ± SEM). Serum levels of IgA-IgG2a immune complexes before injection of cells were 0.079±0.005.
[d]Serum levels of BUN 3 weeks after implantation of 6-19 or 46-42 IgA RF–secreting cells, expressed as mg/dl (mean of 7–10 mice ± SEM). Serum levels of BUN before injection of cells were 22.6±2.1 mg/dl.
[e]As evaluated by histologic examination.

cannot form IgA-IgG2a immune complexes, failed to develop appreciable histologic alterations of glomeruli (Figure 2E and Supplemental Figure 1). Their glomeruli displayed a certain extent of IgA deposits but no significant C3 deposits, suggesting the contribution of complement activation to the development of the 6-19 model of GN. This was confirmed in C3-deficient BALB/c mice, in which 6-19 IgA RF was unable to induce significant glomerular lesions despite substantial glomerular deposits of IgA and IgG2a (Figure 2F and Supplemental Figure 1). Notably, levels of BUN remained low in immunoglobulin- or C3-deficient BALB/c mice implanted with 6-19 IgA–secreting cells, whereas serum levels of IgA anti-IgG2a RF were similar to those observed in wild-type mice receiving 6-19 IgA cells (Table 1). These results strongly suggest that the formation of IgA-IgG2a immune complexes and subsequent activation of complement are critical for the development of 6-19 IgA RF–induced glomerular lesions.

Similar Proportion of Polymeric and Monomeric Forms of 6-19 and 46-42 IgA RF mAbs

Because IgA can be secreted in polymeric or monomeric form, and because a polymeric form of IgA could be more nephritogenic, we determined the proportion of polymeric and monomeric forms of 6-19 and 46-42 IgA RF mAbs. For this purpose, purified 6-19 and 46-42 IgA RF mAbs were subjected to Sephadex G200 gel filtration chromatography to compare the elution profile of these two IgA RF mAbs. Two peaks of IgA were identified for both IgA RF mAbs, with the first peak corresponding to the polymeric form of IgA and the second peak eluted at the volumes characteristic for monomers (Figure 3). Relative concentrations of polymeric versus monomeric IgA were similar between 6-19 and 46-42 IgA RF mAbs, indicating that 6-19 IgA did not display a particularly high proportion of polymeric IgA. Notably, 6-19 and 46-42 anti-IgG2a RF activities were associated only with the first peak of polymeric IgA but not with fractions containing monomeric form of IgA (Figure 3), indicating a low-affinity feature of both RF mAbs. In addition, we observed that the analysis of anti-IgG2a RF activities by serially diluted polymeric forms showed no significant differences between these two IgA RF mAbs (data not shown).

High Levels of Galactosylated *O*-Linked Glycans in the Hinge Region of 6-19 IgA Anti-IgG2a RF mAb

Investigators of a previous study speculated that the first threonine residue at position 228 in the hinge region (PTPPPPITIPSC) of murine IgA bearing the *Igh-2*^{a} allotype could be a potential *O*-linked glycosylation site.[12] Both 6-19 and 46-42 IgAs carry the *Igh-2*^{a} allotype because the Cα gene derived from BALB/c mice (*Igh-2*^{a}) was used for the generation of 6-19 IgA and because 46-42 IgA RF hybridoma was established from MRL-*Fas*^{lpr} mice carrying the same IgA allotype. The cDNA nucleotide sequences of constant regions of both IgA mAbs indeed confirmed their identity to the IgA constant region of BALB/c mice (GenBank accession number: D11468).[20] Furthermore, this analysis excluded the presence of potential *O*- and *N*-linked glycosylation sites in variable regions of their heavy and light chains (Supplemental Figure 2).

To determine whether the observed different pathogenic activities of 6-19 and 46-42 IgA RF mAbs could be attributable to possible structural differences in the carbohydrate side chains attached to the IgA Fc region, we first explored the presence of *O*-glycans in the hinge region of IgA RF mAb. The peptide fraction containing the 62–amino acid hinge peptide of each IgA mAb obtained by treatment with trypsin and lysylendopeptidase (Figure 4) was collected by HPLC and subjected to matrix-assisted laser desorption/ionization-time-of-flight mass spectrometry (MALDI-TOF MS). The analysis of 6-19 IgA RF mAb identified, in addition to a peak containing the nonglycosylated hinge peptide at m/z 6627, four additional peaks of *O*-glycosylated hinge peptides, which contained GalNAc monosaccharide, GalNAc-Gal disaccharide, and its mono- and disialylated forms (Figure 5). The prevailing form of the carbohydrate composition of *O*-glycans was GalNAc-Gal disaccharide at m/z 6992, and the abundance of the glycosylated peptide ions at this peak was similar to that of the nonglycosylated

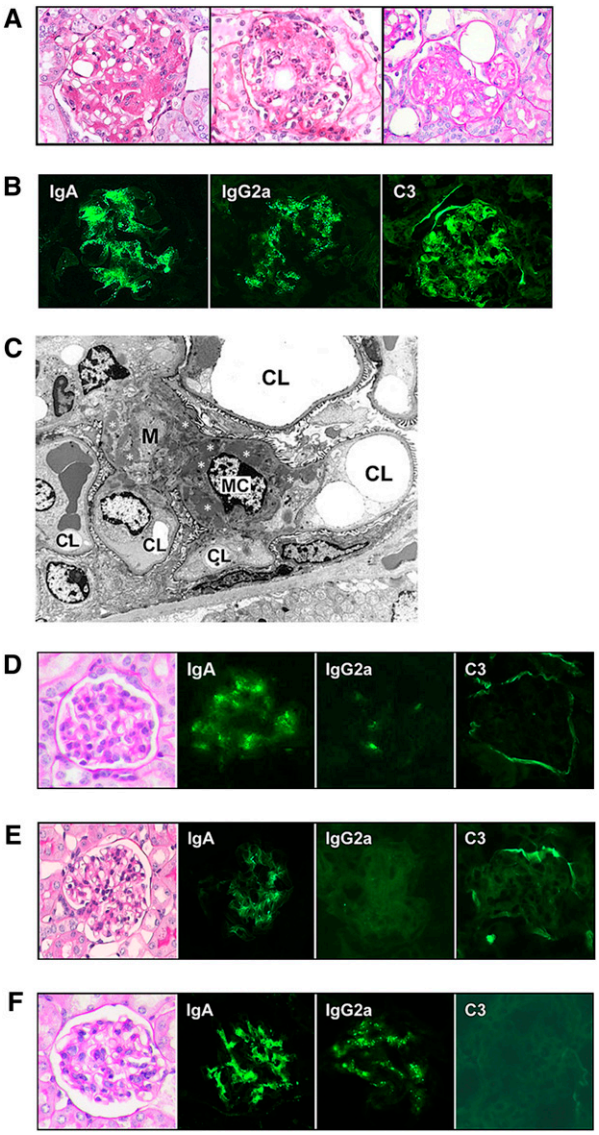

Figure 2. Histologic appearance and immune deposits in BALB/c mice implanted with 6-19 or 46-42 IgA RF–secreting cells and in immunoglobulin- or C3-deficient BALB/c mice implanted with 6-19 IgA RF–secreting cells. (A) Representative glomerular lesions of BALB/c mice implanted with 6-19 IgA RF transfectoma. Note segmental expansion of mesangial matrix and focal proliferation of mesangial cells (left), infiltrations of PMNs (center), and sclerotic changes (right) (periodic acid–Schiff staining; original magnification, ×400). (B) Immunohistochemical analysis of glomerular lesions of BALB/c mice implanted with 6-19 IgA RF transfectoma. Note fine granular deposits of IgA, IgG2a, and C3 in the mesangium (original magnification, ×400). (C) Electron microscopic findings of glomerular lesions in BALB/c mice implanted with 6-19 IgA RF transfectoma. Note prominent electron-dense deposits (indicated by white asterisks) within the mesangium (M). CL, capillary lumen; MC, mesangial cell (original magnification, ×1950). (D) Representative glomerular appearance and immune deposits in BALB/c mice implanted with 46-42 IgA RF hybridoma. Note essentially normal histologic appearance of glomeruli (periodic acid-Schiff staining) and only minimal extent of IgA, IgG2a, and C3 deposits in glomeruli (original magnification, ×400). (E) Representative glomerular appearance and immune deposits in immunoglobulin-deficient BALB/c mice implanted with 6-19 IgA RF transfectoma. Note essentially normal histologic appearance of glomeruli (periodic acid-Schiff staining) and the lack of C3 deposits (original magnification, ×400). (F) Representative glomerular appearance and immune deposits in C3-deficient BALB/c mice implanted with 6-19 IgA RF transfectoma. Note essentially normal histologic appearance of glomeruli (periodic acid-Schiff staining) despite substantial deposits of IgA and IgG2a (original magnification, ×400).

ones. In contrast, the extent of *O*-linked glycosylation in the hinge region of 46-42 IgA RF was obviously low, as demonstrated by the relative abundance of the glycopeptide ions (approximately 15% of unglycosylated species), the carbohydrate composition of which was GalNAc-Gal disaccharide or its monosialylated form (Figure 5).

Difference in the Structure of *N*-Glycans in the CH1 Domain between 6-19 and 46-42 IgA Anti-IgG2a RF mAbs

The structure of *N*-glycans are classified into three main categories—high mannose-, hybrid- or complex-type—all of which share the common core structure Manα1-3(Manα1-6) Manβ1-4GlcNAcβ1-4GlcNAc-Asn (Man: mannose; GlcNAc: *N*-acetylglucosamine; Asn: asparagine), but differ in their outer branches.[21] Several studies reported that reduced or absent galactosylation of *N*-glycans of murine IgA was associated with the development of IgAN-like glomerular lesions.[14–16] Therefore, we compared the structure of *N*-linked oligosaccharide side chains present in CH1 and CH3 domains of 6-19 and 46-42 IgA RF mAbs. MALDI-TOF MS analysis revealed the presence of three *N*-glycans, one at Asn position 162 (N162) in CH1 and two at N438 and N453 in CH3 of both IgA RF mAbs (Figure 4), with the carbohydrate compositions of the *N*-glycans in the CH1 and CH3 domains being highly different. The CH1 domain of 6-19 IgA RF mAb carried *N*-linked bi- and triantennary complex-type oligosaccharide chains (Figure 6). Significantly, the major glycans were of the biantennary type, with arms terminating with GlcNAc-Gal plus one or two sialic acids (*i.e.*, highly galactosylated) and with core fucose (m/z 6365 and 6672). The sialylated species were confirmed by the mass shift corresponding to *N*-glycolylneuraminic acid (Neu5Gc) after acetic acid treatment (data not shown). In contrast, *N*-glycans in the CH1 domain of 46-42 IgA RF mAb displayed the hybrid-type structure, which has features of both high mannose- and complex-type oligosaccharides (Figure 6). The glycoforms attached to the two *N*-linked glycosylation sites (N438 and N453) in the CH3 domain of 6-19 IgA were similar to those of 46-42 IgA. *N*-glycans at position 438 had a mixed composition of high mannose- and complex-type (bi- and triantennary) oligosaccharide chains (Figure 7). Again, complex-type oligosaccharide chains found in 6-19 IgA as well as 46-42 IgA were largely galactosylated, whereas the fucosylation levels were higher in 6-19 IgA. In contrast, *N*-glycans at position

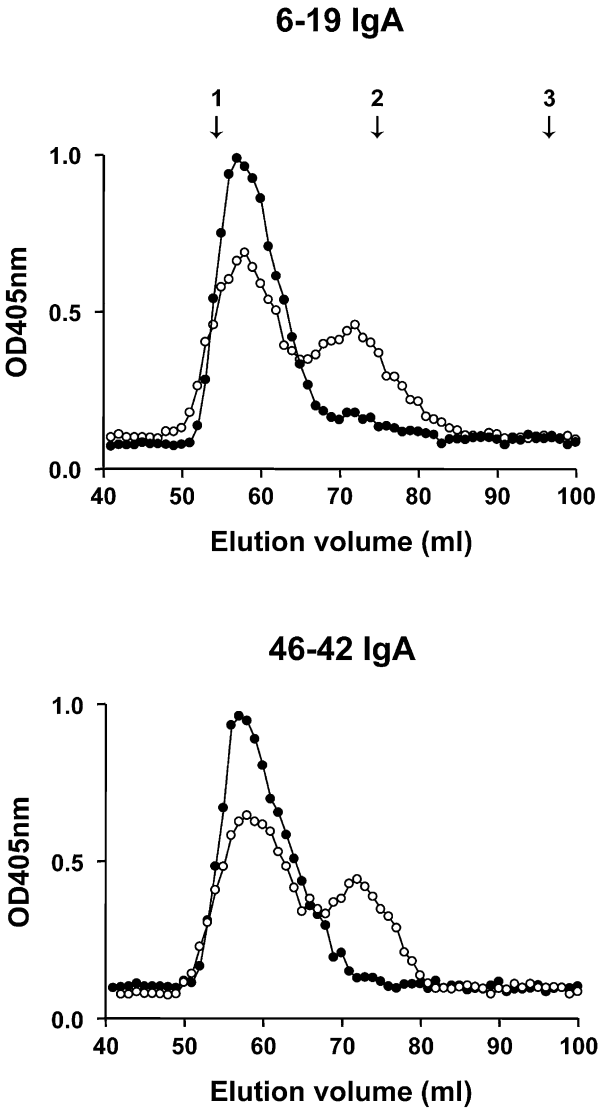

Figure 3. Elution profiles of 6-19 and 46-42 IgA RF mAbs on Sephadex G200 gel filtration column. Relative concentrations of IgA (open circle) and IgA anti-IgG2a RF (closed circle) in each fraction, expressed as OD values at 405 nm, were estimated by ELISA. The column was calibrated with blue dextran (void volume), IgG (150 kD), and BSA (67 kD), the positions of which are indicated by arrows: 1, void volume; 2, IgG; 3, BSA.

453 were exclusively of high mannose-type in both IgAs (Supplemental Figure 3).

DISCUSSION

The present study was designed to assess the nephritogenic potential of two different IgA anti-IgG2a RF mAbs (6-19 and 46-42) bearing the same IgA allotype (*Igh-2*^{a}) and to correlate this potential with the structural differences of the *O*- and *N*-linked oligosaccharide chains attached to the Fc region of IgA. We demonstrate that only 6-19 IgA mAb is able to induce severe glomerular lesions resembling human IgAN. Strikingly, in contrast to 46-42 IgA, 6-19 IgA is highly *O*-glycosylated in its hinge region; this proves (for what we believe to be the first time) the presence of the *O*-linked glycosylation site in the hinge region of mouse IgA.

The lack of glomerular lesions in immunoglobulin- and C3-deficient mice despite the presence of mesangial deposits of IgA and a limited extent of IgA deposits in mice injected with 46-42 IgA hybridoma despite the presence of high levels of IgA-IgG2a immune complexes suggest that the development of 6-19 IgA RF-induced glomerular lesions depends on the formation and mesangial deposition of IgA-IgG2a immune complexes and subsequent activation of complement. The absence of C3 deposits in immunoglobulin-deficient mice implanted with 6-19 IgA–secreting cells is in agreement with our recent finding that mouse IgA is unable to activate complement.[22] Because mouse IgG2a is a potent activator of complement *in vivo*, it is likely that the activation of complement following mesangial localization of IgA-IgG2a immune complexes could trigger glomerular inflammation, thereby contributing to the development of glomerular lesions in this model.

Our demonstration of massive mesangial deposits of IgA, together with IgG2a and C3, in the 6-19 murine model of GN suggests a possible contribution of IgA RF-IgG immune complexes to the development of human IgAN. This is in line with the observation that increases in serum levels of IgA RF have been reported in approximately 50% of patients with IgAN.[2,23] Nevertheless, possible differences between human and experimental murine forms of IgA GN also deserve consideration. Although serum levels of IgA-IgG2a immune complexes were significantly correlated with the severity of IgAN-like glomerular lesions occurring in a high-IgA strain of ddY mice,[24] our preliminary analysis failed to detect the presence of IgA anti-IgG2a RF in sera of these mice. Notably, the implication of alternative IgA-IgG immune complex systems has been suggested in human IgAN, in which the formation of IgA1-IgG immune complexes could be induced as a result of interaction of neoantigenic GalNAc exposed on the hypogalactosylated *O*-glycans of IgA1 with naturally occurring IgG antibodies.[4,25]

It is striking that 46-42 IgA anti-IgG2a RF, which has the same IgA allotype as 6-19 IgA RF, failed to induce glomerular lesions. Notably, the proportion of polymeric versus monomeric forms and the IgG2a-binding affinity of 46-42 IgA RF were similar to those of 6-19 IgA RF, and serum levels of IgA RF and IgA-IgG2a immune complexes in 46-42 implanted mice were even higher than those of mice implanted with 6-19 IgA RF–secreting cells. Thus, the distinct nephritogenic potential of 6-19 versus 46-42 IgA RF mAb could be attributed to the difference observed in the structures of oligosaccharide side chains attached to IgA. Indeed, only 6-19 IgA RF was highly *O*-glycosylated in its hinge region, consistent with finding that the occupancy of the *O*-linked glycosylation site is partial in human IgA1.[10,11] The attachment of GalNAc to serine or threonine is catalyzed by UDP-*N*-acetylgalactosaminyl transferases (GalNAcT); a study in human B cells reported that among the six GalNAcTs expressed

```
125                                                 162
esarnptiypltlppalssdpviigclihdyfpsgtmnvtwgksgkdittvnfppalasg

185                                                       228
grytmssqltlpavecpegesvkcsvqhdsnpvqeldvncsgptpppitipscqpslsl

245
qrpaledlllgsdasitctlnglrnpegavftwepstgkdavqkkavqnscgcysvssvl

305
pgcaerwnsgasfkctvthpesgtltgtiakvtvntfppqvhllpppseelalnellslt

365
clvrafnpkevlvrwlhgneelspesylvfeplkepgegattylvtsvlrvsaetwkqgd

425             438                 453
qyscmvghealpmnftqktidrlsgkptnvsvsvimsegdgicy
```

Figure 4. Predicted amino acid sequences of constant region of 6-19 and 46-42 IgA mAbs bearing the *Igh-2*^{a} allotype. The 62–amino acid hinge peptide of each IgA mAb yielded by treatment with trypsin and lysylendopeptidase is underlined, in which the hinge region is highlighted in gray. The potential *O*-linked glycosylation site at threonine position 228 and three *N*-linked glycosylation sites at N162, N438, and N453 are boxed.

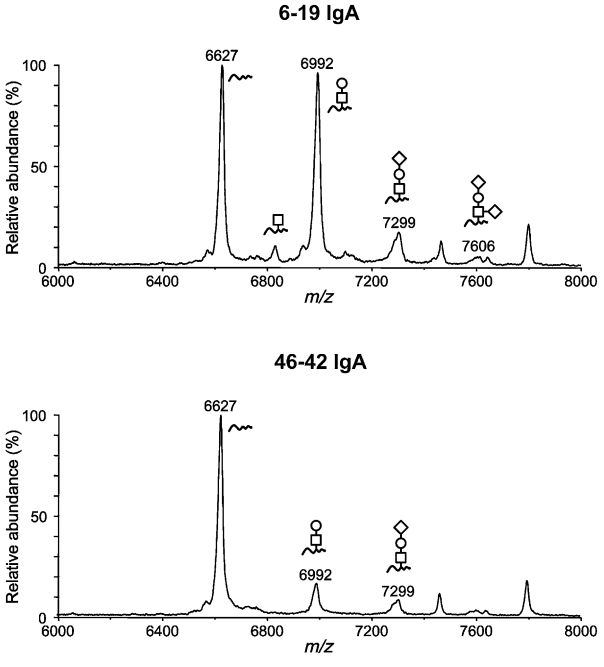

Figure 5. MALDI linear-TOF mass spectra of glycopeptides bearing *O*-glycans from the hinge region of 6-19 and 46-42 IgA RF mAbs. The glycoforms are indicated above the corresponding glycopeptide peaks (open square, GalNAc; open circle, Gal; open diamond, Neu5Gc). Peaks without indication of glycoforms were derived from other peptides. m/z, mass-to-charge ratio.

in these cells, GalNAcT2 exhibited the highest catalytic activity in transferring GalNAc to a synthetic peptide corresponding to the hinge region of human IgA1.[26] In agreement with this finding, our ongoing analysis showed approximately eightfold higher levels of GalNAcT2 mRNA in 6-19 transfectomas than in 46-42 hybridoma cells. Using these two IgA-secreting cells to modulate the expression of GalNAcT2, we should be able to formally prove that GalNAcT2 is indeed the enzyme responsible for the initiation of *O*-glycosylation of the hinge region of mouse IgA.

Our studies also showed that the structure of *N*-glycans attached to the CH1 domain of pathogenic 6-19 IgA mAb is markedly different from that of nonpathogenic 46-42 IgA mAb: bi- and trianternnary complex-type oligosaccharides chains in 6-19 IgA versus hybrid-type oligosaccharides in 46-42 IgA. In contrast, we did not find substantial differences in *N*-glycan's structures present in the CH3 domain between these two RF mAbs, except increased fucosylation of 6-19 IgA. However, it should be stressed that *N*-linked complex-type oligosaccharides present in CH1 and CH3 domains of 6-19 IgA were highly galactosylated. These data indicate that Gal deficiency in *N*-glycans of IgA is not essential for the development of the 6-19 model of GN, although Gal deficiency of serum IgA has previously been reported to be associated with the development of glomerular lesions in other murine models of IgAN.[14–16]

The possibility of a critical pathogenic role of *O*-glycans present in the 6-19 IgA hinge region for the development of glomerular lesions remains to be tested. It should be stressed that 6-19 IgA *O*-glycans were highly galactosylated, in contrast to the hypogalactosylated *O*-glycans of IgA1 in patients with IgAN. Nevertheless, it can be speculated that differences in the oligosaccharide structures of 6-19 IgA RF mAb could lead to a conformational change in the Fc region, thereby promoting an increased mesangial deposition of IgA-IgG2a immune complexes. The extent of *O*-linked glycosylation and galactosylation of 6-19 or 46-42 IgA RF mAbs could be reduced or enhanced through modulation of the expression levels of enzymes respectively essential for initiation of *O*-linked glycosylation or the subsequent addition of Gal residue, or through the introduction of mutations in the hinge region. We should then be able to address the still unsolved question of whether glycosylation of *O*-glycans in the IgA1 hinge region plays a critical role for the development of IgAN. Clearly, our new experimental model of GN induced by 6-19 IgA RF mAb should help not only to improve our understanding of the immunopathologic mechanisms involved in the development of IgAN but also to identify molecules central to the development of human IgAN. This could provide us with promising new targets for the design of novel therapeutic strategies for immune nephropathy.

CONCISE METHODS

Mice

BALB/c mice were purchased from the Jackson Laboratory (Bar Harbor, ME). Immunoglobulin-deficient BALB/c μMT mice, backcrossed for 10 generations on a BALB/c background, were a gift of

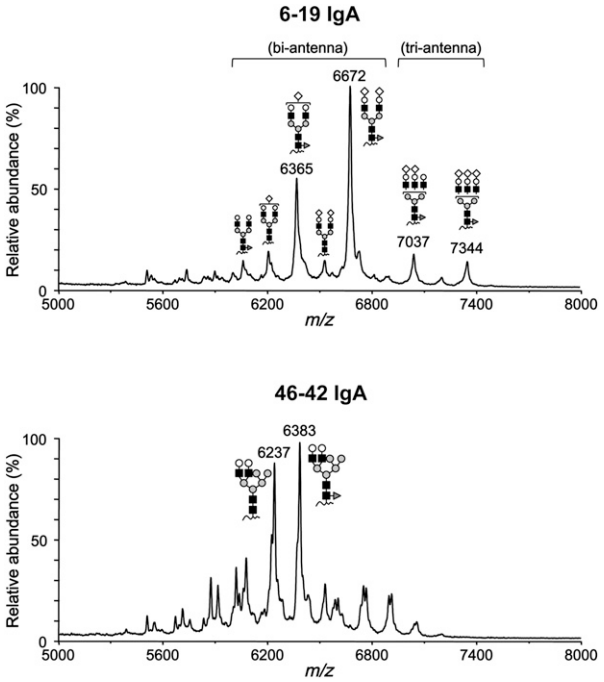

Figure 6. MALDI linear-TOF mass spectra of glycopeptides bearing *N*-glycans attached to N162 in the CH1 domain of 6-19 and 46-42 IgA RF mAbs. The glycoforms are indicated above corresponding glycopeptide peaks. Note that the glycoforms in 6-19 IgA were bi- and triantennary complex types, whereas the glycoforms in 46-42 IgA were hybrid type (closed square, GlcNAc; gray circle, mannose; open circle, Gal; open diamond, Neu5Gc; dark gray triangle, fucose). Peaks without indications of glycoforms were derived from other peptides.

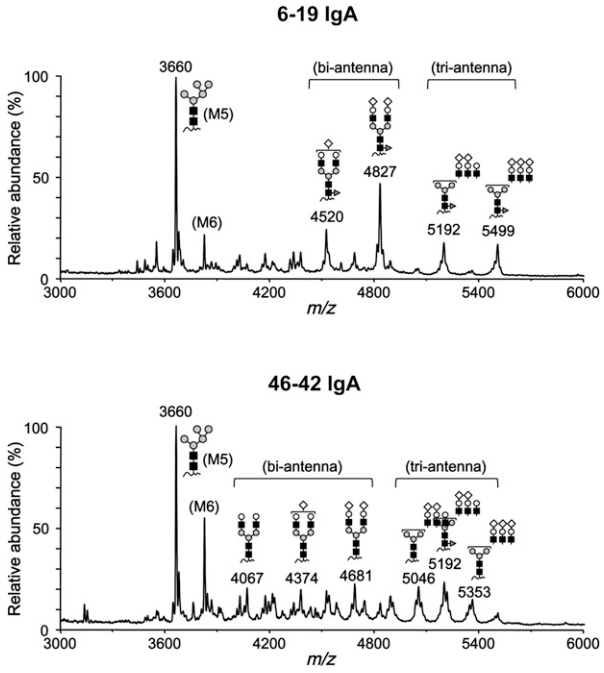

Figure 7. MALDI linear-TOF mass spectra of glycopeptides bearing *N*-glycans attached to N438 in the CH3 domain of 6-19 and 46-42 IgA RF mAbs. The glycoforms are indicated above corresponding glycopeptide peaks. Note the presence of bi- and triantennary complex-types and high mannose-type glycoforms in both 6-19 and 46-42 IgA (closed square, GlcNAc; gray circle, mannose; open circle, Gal; open diamond, Neu5Gc; dark gray triangle, fucose). Peaks without indications of glycoforms were derived from other peptides. M5 and M6 indicate the high mannose-type oligosaccharides containing five and six mannose residues, respectively.

Dr. Pascal Launois, University of Lausanne, Switzerland.[27] C3-deficient mice[28] were backcrossed for six generations on a BALB/c background. Animal studies described in the present study have been approved by the Ethics Committee for Animal Experimentation of the Faculty of Medicine, University of Geneva.

DNA Construction

The VDJ6-19-Cα plasmid containing the complete 6-19 heavy-chain gene of IgA class was constructed using the following DNA fragments: the rearranged VDJ region isolated from cDNA encoding the variable region of the heavy chain of the 6-19 mAb,[29] the promoter region from pSV-Vμ1,[30] the heavy-chain enhancer region from pSVE2-neo,[31] and the Cα region from the genomic clone pIgα-8 isolated from BALB/c mice.[32]

mAb

The 6-19 IgG3 and 46-42 IgA anti-IgG2a RF mAbs were established from unimmunized MRL-*Fas*^{lpr} mice.[33,34] The 6-19 IgA class-switch variant was obtained by transfecting 6-19 heavy-chain-loss mutant cells by electroporation with the VDJ6-19-Cα plasmid together with a pSVE2-neo plasmid containing the neomycin-resistant gene, as described elsewhere.[35] IgA mAb was purified from culture supernatants by an affinity column coupled with 11.44 rat anti-mouse IgA mAb.

Implantation of Transfectoma or Hybridoma Cells

To study the nephritogenicity of IgA anti-IgG2a RF mAb, 10^7 transfectoma or hybridoma cells secreting IgA anti-IgG2a RF mAb were injected intraperitoneally into pristine-treated BALB/c mice that were sacrificed when moribund. To avoid rejection of the transfectoma or hybridoma cells, immunosuppression was achieved by a simultaneous injection of a mixture of anti-mouse CD4 (GK1.5) and anti-mouse CD8 (H-35) mAb (0.5 mg of each mAb), as described elsewhere.[36] Kidneys were obtained at autopsy, processed for histologic examination, and stained with periodic acid–Schiff. Glomerular deposition of IgA and IgG2a was determined by staining frozen kidney sections with rat anti-IgA (11.44) or anti-IgG2a (Ig(1a)8.3) mAb, followed by FITC-labeled goat anti-rat Ig conjugates (Vector Laboratories, Inc., Burlingame, California). C3 deposits were examined by direct staining with anti-mouse C3 conjugates (Cappel Laboratories, West Chester, PA). Parts of the kidneys were fixed in 20% glutaraldehyde, embedded in Epon, and stained with osmium for ultrastructural examination, performed with a Philips EM 400T electron microscope (Rotterdam, the Netherlands).

Serologic Assay

Serum levels of IgA anti-IgG2a RF were determined by ELISA as described elsewhere.[37] Briefly, microtiter plates were coated with TNP8-BSA and subsequently incubated with Hy1.2 IgG2a anti-TNP

mAb before the addition of serum samples. The assay was developed with alkaline phosphatase–labeled 11.44 rat anti-mouse IgA mAb. Results are expressed as μg of IgA anti-IgG2a per ml by referring to a standard curve obtained from purified 6-19 IgA anti-IgG2a RF mAb. Serum concentrations of IgA-IgG2a immune complexes were quantified by ELISA, in combination with precipitation of serum by polyethylene glycol (Siegfried Zofingen, Switzerland). Briefly, 5 μL of serum samples were treated for 1 hour at 4°C with 10% of polyethylene glycol, which allowed precipitation only of IgA RF-IgG2a immune complexes, not free IgG2a. The precipitates were washed twice with polyethylene glycol and solubilized in 1% BSA-PBS-0.05% Tween 20. Then, samples were subjected to ELISA using plates coated with goat anti-mouse IgA (Bethy Laboratories, Inc., Cambridge, United Kingdom), and the assay was developed with alkaline phosphatase–labeled goat anti-mouse IgG2a conjugates (Southern Biotechnology Associates, Inc., Birmingham, AL). Results are expressed as OD at 405 nm. BUN and serum creatinine were measured by autoanalyzer (Fuji Dry-chem 5500, Fujifilm, Tokyo, Japan).

Gel Filtration

The size distribution of IgA anti-IgG2a RF mAb was analyzed using a Sephadex G200 gel filtration column (Pharmacia, Uppsala, Sweden) equilibrated with 50 mM phosphate buffer (pH, 7.4) containing 0.15 M NaCl, and elution was performed using the same buffer at a flow rate of 0.2 ml/min at 4°C. The column was calibrated with blue dextran (void volume), IgG (150 kD), and BSA (67 kD). Relative concentrations of IgA and IgA anti-IgG2a RF in each fraction were estimated by ELISA.

Reverse Transcriptase PCR and cDNA Sequencing

RNA from 46-42 hybridoma cells was purified with TRIzol reagent (Invitrogen AG, Basel, Switzerland). For nucleotide sequencing of the entire variable and constant regions of the heavy and light chains of 46-42 IgA anti-IgG2a RF mAb, cDNA was amplified with *Pfu* DNA polymerase (Stratagene Cloning Systems, La Jolla, CA) using the following pairs of primers: (*1*) VH1BACK forward primer (5′-AGGTSMARCTGCAGSAGTCWGG-3′)[38] and 3′-UT Cα reverse primer (5′-GAAGTGCAGGGATACTTTGG-3′) for the heavy chain and (*2*) V*k*1BACK forward primer (5′-GACATTCAGCTGACCCAGTCTCCA-3′)[38] and C*k* reverse primer (5′-TGTTCAAGAAGCACACG-3′) for the light chain.

Analysis of Oligosaccharide Structures

The oligosaccharide profiles were analyzed by the MALDI linear-TOF MS of glycopeptides according to the method described elsewhere.[11,39] Briefly, IgA mAbs were reduced by dithiothreitol and carboxamidomethylated with iodoacetamide in a solution of 6 M guanidium chloride, 0.25 M Tris-HCl, and 1 mM EDTA (pH, 8.0). The alkylated proteins were desalted with a NAP-5 gel filtration column (GE Healthcare, Buckinghamshire, United Kingdom) equilibrated with 0.05 M HCl. The pH was then adjusted to 8.5 by titration with a 1.5-M Tris solution for digestion, which was performed with a mixture of trypsin (Promega, Buckinghamshire, United Kingdom) and lysylendopeptidase (Wako, Osaka, Japan). Peptides in the digest were separated by HPLC using a 1.0 mm $\times$ 150 mm C8 reversed phase column (Inertsil WP300, GL Science, Tokyo, Japan) with a linear gradient of acetonitrile in 0.1% (vol/vol) trifluoroacetic acid. Glycopeptides in the elution fractions were identified and characterized by MALDI MS using a Voyager DE Pro time-of-flight mass spectrometer (Applied Biosystems, Foster City, CA), which was operated in the linear mode. The sample matrix was 2,5-dihydroxybenzoic acid, which was dissolved in 50% (vol/vol) acetonitrile at a concentration of 10 mg/ml. An aliquot of an HPLC fraction was mixed with a dihydroxybenzoic acid solution on the MALDI sample target.

Statistical Analyses

Unpaired comparisons of serologic parameters were analyzed by *t* test. $P>0.05$ was considered to represent insignificant differences.

ACKNOWLEDGMENTS

We thank Dr. Yusuke Suzuki for the analysis of BUN and creatinine; Ms. Céline Manzin Lorenzi, Ms. Montserrat Alvarez, and Mr. Guy Brighouse for excellent technical assistance; and Dr. Thomas Moll for critically reading the manuscript.

This work was supported by grants from the Swiss National Foundation for Scientific Research, EMBO Fellowship, the Novaritis Foundation, and la Fondation pour la Recherche Médicale and by a Grant-in-Aid for Scientific Research (B) (19390093 and 23390081).

DISCLOSURES

None.

REFERENCES

1. Donadio JV, Grande JP: IgA nephropathy. *N Engl J Med* 347: 738–748, 2002
2. Czerkinsky C, Koopman WJ, Jackson S, Collins JE, Crago SS, Schrohenloher RE, Julian BA, Galla JH, Mestecky J: Circulating immune complexes and IgA rheumatoid factor in patients with mesangial IgA nephropathies. *J Clin Invest* 77: 1931–1938, 1986
3. Baenziger J, Kornfeld S: Structure of the carbohydrate units of IgA1 immunoglobulin. II. Structure of the *O*-glycosidically linked oligosaccharide units. *J Biol Chem* 249: 7270–7281, 1974
4. Tomana M, Novak J, Julian BA, Matousovic K, Konecny K, Mestecky J: Circulating immune complexes in IgA nephropathy consist of IgA1 with galactose-deficient hinge region and antiglycan antibodies. *J Clin Invest* 104: 73–81, 1999
5. Allen AC, Bailey EM, Barratt J, Buck KS, Feehally J: Analysis of IgA1 *O*-glycans in IgA nephropathy by fluorophore-assisted carbohydrate electrophoresis. *J Am Soc Nephrol* 10: 1763–1771, 1999
6. Hiki Y, Odani H, Takahashi M, Yasuda Y, Nishimoto A, Iwase H, Shinzato T, Kobayashi Y, Maeda K: Mass spectrometry proves under-*O*-glycosylation of glomerular IgA1 in IgA nephropathy. *Kidney Int* 59: 1077–1085, 2001
7. Allen AC, Bailey EM, Brenchley PE, Buck KS, Barratt J, Feehally J: Mesangial IgA1 in IgA nephropathy exhibits aberrant *O*-glycosylation: Observations in three patients. *Kidney Int* 60: 969–973, 2001
8. Young NM, Jackson GE, Brisson JR: The glycopeptides of the mouse immunoglobulin A T15. *Mol Immunol* 27: 1083–1090, 1990
9. Lipniunas P, Grönberg G, Krotkiewski H, Angel AS, Nilsson B: Investigation of the structural heterogeneity in the carbohydrate portion of a mouse monoclonal immunoglobulin A antibody. *Arch Biochem Biophys* 300: 335–345, 1993

10. Mattu TS, Pleass RJ, Willis AC, Kilian M, Wormald MR, Lellouch AC, Rudd PM, Woof JM, Dwek RA: The glycosylation and structure of human serum IgA1, Fab, and Fc regions and the role of *N*-glycosylation on Fc α receptor interactions. *J Biol Chem* 273: 2260–2272, 1998
11. Wada Y, Tajiri M, Ohshima S: Quantitation of saccharide compositions of *O*-glycans by mass spectrometry of glycopeptides and its application to rheumatoid arthritis. *J Proteome Res* 9: 1367–1373, 2010
12. Phillips-Quagliata JM: Mouse IgA allotypes have major differences in their hinge regions. *Immunogenetics* 53: 1033–1038, 2002
13. Robinson EA, Appella E: Complete amino acid sequence of a mouse immunoglobulin α chain (MOPC 511). *Proc Natl Acad Sci U S A* 77: 4909–4913, 1980
14. Kobayashi I, Nogaki F, Kusano H, Ono T, Miyawaki S, Yoshida H, Muso E: Interleukin-12 alters the physicochemical characteristics of serum and glomerular IgA and modifies glycosylation in a ddY mouse strain having high IgA levels. *Nephrol Dial Transplant* 17: 2108–2116, 2002
15. Marquina R, Díez MA, López-Hoyos M, Buelta L, Kuroki A, Kikuchi S, Villegas J, Pihlgren M, Siegrist CA, Arias M, Izui S, Merino J, Merino R: Inhibition of B cell death causes the development of an IgA nephropathy in (New Zealand white x C57BL/6)F1-*bcl-2* transgenic mice. *J Immunol* 172: 7177–7185, 2004
16. Nishie T, Miyaishi O, Azuma H, Kameyama A, Naruse C, Hashimoto N, Yokoyama H, Narimatsu H, Wada T, Asano M: Development of immunoglobulin A nephropathy-like disease in β-1,4-galactosyltransferase-I-deficient mice. *Am J Pathol* 170: 447–456, 2007
17. Lemoine R, Berney T, Shibata T, Fulpius T, Gyotoku Y, Shimada H, Sawada S, Izui S: Induction of "wire-loop" lesions by murine monoclonal IgG3 cryoglobulins. *Kidney Int* 41: 65–72, 1992
18. Fulpius T, Spertini F, Reininger L, Izui S: Immunoglobulin heavy chain constant region determines the pathogenicity and the antigen-binding activity of rheumatoid factor. *Proc Natl Acad Sci U S A* 90: 2345–2349, 1993
19. Abdelmoula M, Spertini F, Shibata T, Gyotoku Y, Luzuy S, Lambert PH, Izui S: IgG3 is the major source of cryoglobulins in mice. *J Immunol* 143: 526–532, 1989
20. Oida E, Nogaki F, Kobayashi I, Kamata T, Ono T, Miyawaki S, Serikawa T, Yoshida H, Kita T, Muso E: Quantitative trait loci (QTL) analysis reveals a close linkage between the hinge region and trimeric IgA dominancy in a high IgA strain (HIGA) of ddY mice. *Eur J Immunol* 34: 2200–2208, 2004
21. Kornfeld R, Kornfeld S: Assembly of asparagine-linked oligosaccharides. *Annu Rev Biochem* 54: 631–664, 1985
22. Baudino L, Fossati-Jimack L, Chevalley C, Martinez-Soria E, Shulman MJ, Izui S: IgM and IgA anti-erythrocyte autoantibodies induce anemia in a mouse model through multivalency-dependent hemagglutination but not through complement activation. *Blood* 109: 5355–5362, 2007
23. Sinico RA, Fornasieri A, Oreni N, Benuzzi S, D'Amico G: Polymeric IgA rheumatoid factor in idiopathic IgA mesangial nephropathy (Berger's disease). *J Immunol* 137: 536–541, 1986
24. Suzuki H, Suzuki Y, Aizawa M, Yamanaka T, Kihara M, Pang H, Horikoshi S, Tomino Y: Th1 polarization in murine IgA nephropathy directed by bone marrow-derived cells. *Kidney Int* 72: 319–327, 2007
25. Suzuki H, Fan R, Zhang Z, Brown R, Hall S, Julian BA, Chatham WW, Suzuki Y, Wyatt RJ, Moldoveanu Z, Lee JY, Robinson J, Tomana M, Tomino Y, Mestecky J, Novak J: Aberrantly glycosylated IgA1 in IgA nephropathy patients is recognized by IgG antibodies with restricted heterogeneity. *J Clin Invest* 119: 1668–1677, 2009
26. Iwasaki H, Zhang Y, Tachibana K, Gotoh M, Kikuchi N, Kwon YD, Togayachi A, Kudo T, Kubota T, Narimatsu H: Initiation of *O*-glycan synthesis in IgA1 hinge region is determined by a single enzyme, UDP-*N*-acetyl-α-D-galactosamine:polypeptide *N*-acetylgalactosaminyltransferase 2. *J Biol Chem* 278: 5613–5621, 2003
27. Ronet C, Hauyon-La Torre Y, Revaz-Breton M, Mastelic B, Tacchini-Cottier F, Louis J, Launois P: Regulatory B cells shape the development of Th2 immune responses in BALB/c mice infected with *Leishmania major* through IL-10 production. *J Immunol* 184: 886–894, 2010
28. Wessels MR, Butko P, Ma M, Warren HB, Lage AL, Carroll MC: Studies of group B streptococcal infection in mice deficient in complement component C3 or C4 demonstrate an essential role for complement in both innate and acquired immunity. *Proc Natl Acad Sci U S A* 92: 11490–11494, 1995
29. Reininger L, Berney T, Shibata T, Spertini F, Merino R, Izui S: Cryoglobulinemia induced by a murine IgG3 rheumatoid factor: Skin vasculitis and glomerulonephritis arise from distinct pathogenic mechanisms. *Proc Natl Acad Sci U S A* 87: 10038–10042, 1990
30. Neuberger MS: Expression and regulation of immunoglobulin heavy chain gene transfected into lymphoid cells. *EMBO J* 2: 1373–1378, 1983
31. Simon T, Rajewsky K: 'Enhancer-constitutive' vectors for the expression of recombinant antibodies. *Nucleic Acids Res* 16: 354, 1988
32. Nishida Y, Kataoka T, Ishida N, Nakai S, Kishimoto T, Böttcher I, Honjo T: Cloning of mouse immunoglobulin ε gene and its location within the heavy chain gene cluster. *Proc Natl Acad Sci U S A* 78: 1581–1585, 1981
33. Gyotoku Y, Abdelmoula M, Spertini F, Izui S, Lambert PH: Cryoglobulinemia induced by monoclonal immunoglobulin G rheumatoid factors derived from autoimmune MRL/MpJ-*lpr/lpr* mice. *J Immunol* 138: 3785–3792, 1987
34. Wolfowicz CB, Sakorafas P, Rothstein TL, Marshak-Rothstein A: Oligoclonality of rheumatoid factors arising spontaneously in *lpr/lpr* mice. *Clin Immunol Immunopathol* 46: 382–395, 1988
35. Fossati-Jimack L, Reininger L, Chicheportiche Y, Clynes R, Ravetch JV, Honjo T, Izui S: High pathogenic potential of low-affinity autoantibodies in experimental autoimmune hemolytic anemia. *J Exp Med* 190: 1689–1696, 1999
36. Trendelenburg M, Fossati-Jimack L, Cortes-Hernandez J, Turnberg D, Lewis M, Izui S, Cook HT, Botto M: The role of complement in cryoglobulin-induced immune complex glomerulonephritis. *J Immunol* 175: 6909–6914, 2005
37. Berney T, Fulpius T, Shibata T, Reininger L, Van Snick J, Shan H, Weigert M, Marshak-Rothstein A, Izui S: Selective pathogenicity of murine rheumatoid factors of the cryoprecipitable IgG3 subclass. *Int Immunol* 4: 93–99, 1992
38. Orlandi R, Güssow DH, Jones PT, Winter G: Cloning immunoglobulin variable domains for expression by the polymerase chain reaction. *Proc Natl Acad Sci U S A* 86: 3833–3837, 1989
39. Wada Y, Dell A, Haslam SM, Tissot B, Canis K, Azadi P, Bäckström M, Costello CE, Hansson GC, Hiki Y, Ishihara M, Ito H, Kakehi K, Karlsson N, Hayes CE, Kato K, Kawasaki N, Khoo KH, Kobayashi K, Kolarich D, Kondo A, Lebrilla C, Nakano M, Narimatsu H, Novak J, Novotny MV, Ohno E, Packer NH, Palaima E, Renfrow MB, Tajiri M, Thomsson KA, Yagi H, Yu SY, Taniguchi N: Comparison of methods for profiling *O*-glycosylation: Human Proteome Organisation Human Disease Glycomics/Proteome Initiative multi-institutional study of IgA1. *Mol Cell Proteomics* 9: 719–727, 2010

See related editorial, "Induction of IgA Deposits and Glomerulonephritis by IgA Rheumatoid Factor," on pages 371–373.

This article contains supplemental material online at http://jasn.asnjournals.org/lookup/suppl/doi:10.1681/ASN.2011070701/-/DCSupplemental.